ELSEVIER

Journal of Applied Geophysics 43 (2000) 5–13

JOURNAL OF APPLIED GEOPHYSICS

www.elsevier.nl/locate/jappgeo

Electromagnetic radiation method water-infusion control in rockburst-prone strata

V. Frid *

The Deichmann Rock Mechanics Laboratory of the Negev, Department of Geological and Environmental Sciences, Ben Gurion University of the Negev, Beersheba, Israel

Received 14 September 1998; accepted 8 July 1999

Abstract

An electromagnetic radiation (EMR) method associated with rock fracture was employed to study water infusion in rockburst-prone coal strata. Measurements of EMR activity during borehole drilling revealed that a hole nearing a stress peak excites a sharp increase in EMR activity. Water pressure increase/decrease excited EMR activity up to the coal stratum transition to residual stress. An absence of EMR activity during water pressure changes could be a criterion for water infusion performance.

Keywords: Electromagnetic radiation; Rockburst; Water infusion; Coal mining

1. Introduction

Rockburst hazards in the mine working face can be eliminated by different methods, for example, large diameter hole drilling, camouflage blasting or water infusion. The performance of each method is usually verified after its completion. In this paper we describe a modern method of water infusion control.

The performance of water infusion on rockburst hazardous coal seams is usually estimated by a volume of so-called 'drilled coal rubble' (DCR): volume of coal pieces fissured by drilling. Volume of fissured coal depends on hole diameter, on drilling rate and on stress level. The first two parameters usually remain constant for a given coal stratum, hence, volume of DCR characterizes the stress level.

During infusion, water 'impregnates' coal near the mine working face. If a forecast hole intersects water saturated zone, it excites a water spouting to the mine working face. Then, DCR turns to a slime, and it becomes impossible to measure the DCR volume.

This situation causes a drilling of an additional forecast hole. However, the existence of several forecast holes (intended to estimate wa-

* Tel.: +972-7-6461-770; fax: +972-7-6472-997; e-mail: vfrid@bgumail.bgu.ac.il

0926-9851/00/$ - see front matter
PII: S0926-9851(99)00029-4

ter infusion performance) diminishes the validity of the water infusion itself because the increase of water pressure sometimes excites its breaching to a neighboring hole. Hence, we have a ''closed cycle'': to estimate performance we need a hole, while the holes negatively influence the performance. The only way to cut this ''Gordian knot'' is to estimate water infusion performance during its execution without drilling holes.

This problem may be tackled only by short-term and non-destructive geophysical methods, for example, the method of electromagnetic radiation (EMR) activity registration.

2. Fundamentals of EMR

EMR from materials fractured under compression was firstly observed in 1933 (Urusovskaja, 1969). This study was followed by numerous others, that aimed at investigating the different EMR aspects (Urusovskaja, 1969; Nitsan, 1977; Gokhberg et al., 1979; Goncharov et al., 1980; Warwick et al., 1982; Ogawa et al., 1985; Cress et al., 1987; Gershenzon et al., 1989; Yamada et al., 1989; Xu et al., 1991; Fujinawa et al., 1992; Yoshino et al., 1993). We briefly summarize some known experimental results: (a) The tensile crack formation excites more intensive EMR than shear cracking (Yamada et al., 1989). (b) The increase of elasticity, strength, and loading rate during uniaxial loading increase EMR amplitude (Gol'd et al., 1975; Nitsan, 1977; Khatiashvili, 1984). (c) The key elastic parameter for EMR characterization during triaxial compression is the Poisson ratio. The lower the Poisson ratio, the harder it is for the material to strain transversally, and hence, the higher is the probability of new fractures (especially parallel to the axis) and of the ensuing EMR. On the other hand, the higher the Poisson ratio, the easier it is for the material to strain transversally, and accordingly, fewer fractures and lower EMR activity should be expected (Frid et al., 1999).

Today, the physical mechanism of EMR is unknown. Several attempts to explain the EMR mechanism include the acceleration and deceleration of dislocations (Perelman and Khatiashvilli, 1981; Golovin and Shibkov, 1986a,b), rupture of bonds (Khatiashvili, 1984; Gershenzon et al., 1985), the movement of charged crack sides (Miroshnishenko and Kuksenko, 1980) and electrical breakdown (discharge between charged crack sides, Gol'd et al., 1975; Enomoto and Chaudhri, 1993). Unfortunately, none of these was able to explain the properties of the detected EMR (King, 1983; Rabinovitch et al., 1995, 1996).

Rabinovitch et al. (1998) maintained that the EMR pulse amplitude increases as long as the crack continues to grow, when new atomic bonds are severed and their contribution is added to the EMR. When the crack halts, the pulse amplitude starts to decay. A careful EMR pulse parameterization allowed to associate some EMR parameters with crack dimensions. Thus, the time from the start of the pulse up to its maximum is proportional to the number of severed atomic bonds and thus to the crack length, while the frequency of the EMR pulse relates to the crack width (Rabinovitch et al., 1998, 1999).

During the 1970s and 1980s, the interest in EMR moved from the ''basic'' to the ''applied'' sphere, in connection with problems of earthquake prognosis (e.g., Gokhberg et al., 1979; King, 1983; Gershenzon et al., 1985; Yoshino et al., 1993) and rockburst hazard forecast (e.g., Khatiashvili, 1984; Nesbitt and Austin, 1988; Frid, 1990).

3. EMR registration in underground mines

Khatiashvili (1984) carried out an investigation of EMR in the Tkibulli deep shaft (Georgia) prior to the earthquake of magnitude of 5.4. The registration point (at the shaft position) was located at a distance of 250 km from the

earthquake epicenter. Prior to the earthquake itself, an increase of intensity of the lower part of the spectrum (1–100 kHz) and a corresponding decrease of intensity of higher frequencies (100–1000 kHz) were observed. This phenomenon could, perhaps, be explained by an increase of the number and the sizes of cracks during the earthquake approach.

Nesbitt and Austin (1988) registered EMR activity increase corresponding to micro seismic events (magnitude of -0.4) in a gold mine excavation (2.5 km depth). The amplitude of this EMR signal was about 1.2 μV/m, and it appeared a few seconds prior to the seismic event.

Registration of EMR activity in mine workings of the Ural bauxite deposit showed (Scitovich and Lazarevich, 1985) that its values sharply increased due to rockburst hazard increase. Analogous works in Noril'sk polymetal deposit (Krasnoyarsk region) revealed an increase of EMR amplitude (up to 150–200 μV/m) and activity in the rockburst hazardous zones (Red'kin et al., 1985).

Markov and Ipatov (1986) investigating EMR activity changes in apatite underground mine (Khibin deposit, Kola peninsula) found out that EMR amplitude in rockburst hazardous zones was in the range of 8–25 mV/m and EMR activity here was significantly higher than regular noise level.

EMR investigations in different rockburst and rock and gas outburst situations were carried out in underground coal mines (North Kuzbass deposit) (Frid et al., 1992; Frid, 1997a,b). The EMR activity was measured by a 100-kHz (± 1 kHz) resonance magnetic antenna. After registrations of EMR activity, the degree of rockburst hazard at a given point of mine working was determined by a volume of DCR. These investigations showed that an increase of rockburst hazard, accompanied by an increase of EMR activity, occurs when pillars are found above a given seam, geological faults exist in the area and/or seam thickness sharply diminishes.

4. An employment of EMR for water-infusion control

4.1. Rockburst safety condition

As shown by Petukhov and Lin'kov (1983), rockburst safety condition is the following:

$$\begin{cases} P_{\mathrm{n}} < P_{\mathrm{m}} \\ \dfrac{M_{\mathrm{c}}}{E_{\mathrm{r}}}\dfrac{a_{\mathrm{n}}}{h} < 1 \end{cases} \tag{1}$$

where P_{n} is the external applied load, P_{m} is the limiting load (strength), M_{c} is the coal drop modulus (descending modulus of stress–strain curve beyond peak point under rigid compression, Fig. 1a), E_{r} is the Young modulus of adjoining rocks, a_{n} is the distance up to peak stress from mine working face, h is the half thickness of coal stratum. If coal is under residual strength (non-hazardous condition), both inequalities are complied: load on given zone is lower than the limiting value (first inequality), and the left side of the second inequality is lower than 1 (drop modulus in the residual strength zone is equal to 0).

4.2. EMR in residual strength zone — sample compression

Goncharov et al. (1980) carried out an EMR study on a rigid press. They loaded concrete samples of $0.55 \times 0.55 \times 0.65$ m dimensions. The EMR activity was measured with a magnetic antenna, that had a resonance frequency of 800 kHz (± 1 kHz). The first significant increase of EMR activity occurred at the post-peak zone (Fig. 1a) under the load of 0.95 σ_{c}, where σ_{c} is the strength limit, while the second rise of EMR activity was noted under a load of 0.9 σ_{c} (in the post-peak zone). Single pulses of EMR accompanied the subsequent decrease of the load until 0.75 σ_{c}. In the zone of residual strength (Fig. 1a), EMR activity was ceased.

EMR studies on a rigid press were also performed on ores and rocks from the Khibin

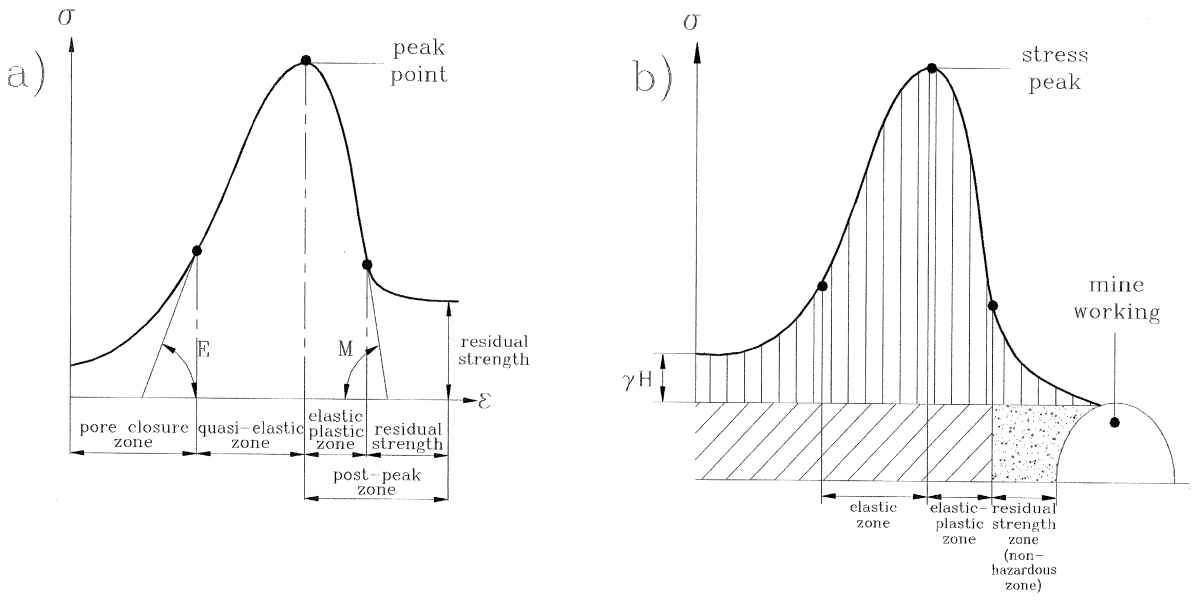

Fig. 1. Typical stress–strain curve during rigid sample compression (a) and stress distribution curve in the zone of mine working influence (b).

apatite deposit (Kola peninsula, Ipatov, 1989), on magnetic ores, granites, white marble and coal from Shpitsbergen (Frid, 1990). EMR activity was registered with 100 kHz (± 1 kHz) resonance magnetic antenna. The maximum EMR activity was measured in the range of 1.0–0.8 σ_c in post-peak zone, while in the zone of residual strength EMR activity was discontinued. The analysis of these results showed that the following EMR features were common for all rocks:

1. A sharp increase of EMR activity in the post-peak zone near the limit of strength.
2. A gradual decrease of EMR activity during the approach to the zone of residual strength.
3. An absence of EMR in the zone of residual strength.

4.3. EMR induced by a borehole drilling

To check these conclusions in situ, we investigated the EMR activity during borehole drilling (hole diameter was 42 mm). Note that the residual strength zone (the last one during sample deformation on rigid stress, Fig. 1a) is the nearest zone to the mine working face (Fig. 1b).

All holes were drilled by 1-m separation interval. During all interval drilling, a cumulative value of EMR activity (summarized value of EMR activity per drilling interval) was measured and after drilling each interval, the DCR value was measured. Forecast drilling in the mine does not generally achieve stress peak due to instrument gripping in a borehole, and stops if DCR volume (stress value) becomes higher than a predetermined value. Forecast drilling (in North Kuzbass mines) is generally conducted up to 6 m depth. Fig. 2 shows two examples of EMR observation during borehole drilling: Fig. 2a — in the rockburst hazardous zone (DCR value is higher than the limiting value, see below) and Fig. 2b — in the non-hazardous zone (DCR value is lower than the limiting value, see below). As is seen from Fig. 2a, DCR value increases up to 12 l/m at the 5th drilling meter, that is significantly higher than limited value (5.5–6 l/m at the 5–6 drilling meter), and hence, forecast drilling was stopped. This

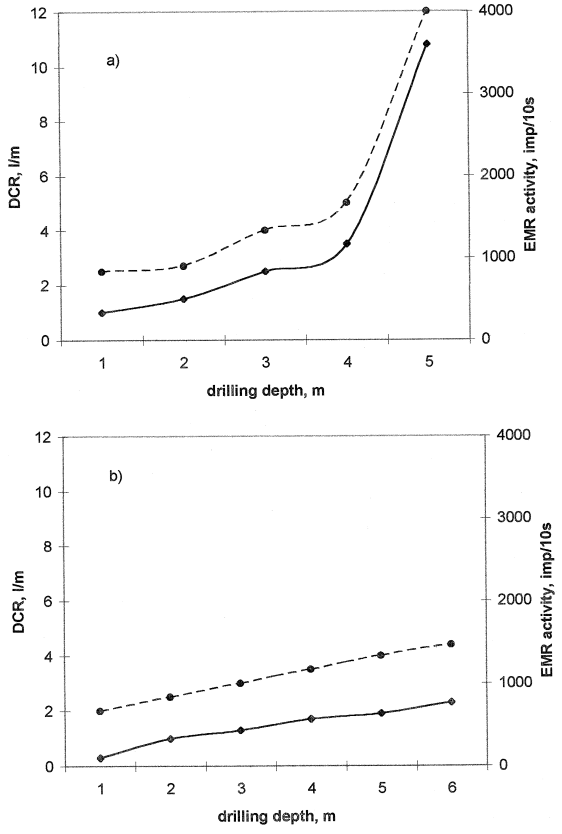

Fig. 2. Two examples of EMR study during forecast drilling: in the rockburst hazardous zone (a) and in the non-hazardous zone (b). Full-drawn curve is the DCR value, while the hatched curve is the EMR activity.

value of DCR evidently indicates the existence of a rockburst hazardous zone at the 5th meter depth from the mine working face. Fig. 2a shows that if a hole face approaches a stress peak (DCR increase above the limiting value), EMR activity sharply increases, and vice versa: if the DCR value does not change drastically (DCR value lower than 5.5–6 l/m at the 5–6 drilling meter — non-hazardous zone, Fig. 2b), EMR activity does not essentially increase.

The analysis of more than 150 drillings conducted on three different coal stratums (Desyatiy, Koksoviy and Andreevskiy) enables us to summarize some general features of EMR activity associated with borehole drilling: (1) The EMR activity sharply increases if hole face approaches a zone of highly stressed coal (that is near the stress peak, e.g., Fig. 2a); (2) The drilling in the non-hazardous zone does not tangibly affect the EMR activity (e.g., Fig. 2b); (3) The EMR activity value induced by drilling is the lowest in the zones nearest to mine working face: zone of crushed coal or by another words zone of residual strength (first drilling meter from mine working face, e.g., Fig. 2a,b).

4.4. Principles of EMR used for water infusion control

The analyses of safety condition (Section 4.1), EMR features induced by sample compression (Section 4.2) and EMR changes associated with borehole drilling (Section 4.3) enables us to state two principles of EMR used for water infusion control:

1. Rockburst is impossible if mine working face is transited to residual strength.
2. If material is under residual strength, its loading is not accompanied by EMR excitation.

5. EMR–water infusion model

As is generally known, rock stress condition may be described by the Coloumb–Mohr envelope (Twiss and Moores, 1992). Let us assume that the coal stress condition in the face of mine working is described by the Mohr circle (Fig. 3,

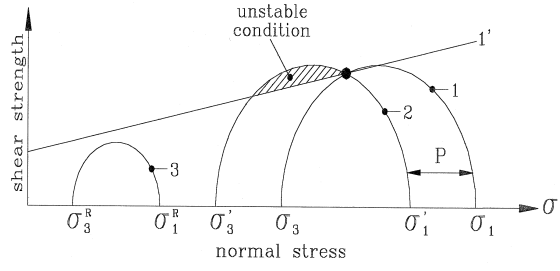

Fig. 3. Mohr–Colulomb failure envelope around Mohr circles which represents the different coal conditions during water infusion.

1) and by the Coloumb–Mohr envelope (Fig. 3, 1′). A water pressure increase forms a pore pressure P that is equivalent to an additive tension stress. This tension stress shifts to the left Mohr circle on P value. Hence, part of the circle will be above the Mohr–Coulomb envelope (Fig. 3, 2), that means coal turns to an unstable condition, and will be fractured. This fracturing results in EMR activity increase. As a result of coal fracturing, its strength will be decreased. However, if stress level in a coal stratum is yet high, a sharp decrease of water pressure (for example, due to pump stopping) will excite crack closure and EMR excitation. Hence, a water pressure cycle (both increase and decrease) will affect EMR activity.

Thus, water pressure changes accompanied by the EMR activity up to the coal transition to residual strength (Fig. 3, 3), and vice versa: an absence of EMR activity variation during water pressure changes during the ''loading–unloading'' cycle could be a criterion of water infusion performance or, in other words, if the coal stratum will be non-hazardous.

6. EMR during water infusion in coal mine

EMR investigations during water infusion were carried out on Koksoviy, Andreevsky, Desyatiy coal stratums North Kuzbass (Russia). Water infusion was conducted in the following manner: (1) The length of the holes was 6 m and the sealed length was 5–5.5 m (a mining experience in North Kuzbass shows that the existence of a 5–6-m safeguard zone (residual strength zone) in mine working face, indicates a non-dangerous condition). (2) Water pressure was increased in a stepwise fashion of 0.2–0.3 γH to provide coal 'impregnation' with water, where γ is the rock density [kg/m^3] and H is the stratum depth [m]. (3) New step of water pressure increase was after EMR activity stabilization. (4) During water infusion, EMR activity was measured by a 100-kHz (± 1 kHz) loop magnetic antenna. The antenna was located 1 m from the mine working face and connected with a special counter (Fig. 4). We measured the number of intersections (per unit time) of the amplitude of oscillated electromagnetic pulses of a given counter sensitivity level. We call this parameter the EMR activity. Each EMR activity reading was taken with a duration of 10 s. For simplicity, we named the unit of EMR activity ''pulse per 10 s'', symbolized as ''pulse/10 s''. (5) After reaching 0.8 γH, water pressure is sharply decreased to 0.3 γH, as our experience shows that if the water pressure exceeds a value of 0.8 γH, the probability of water breaching to mine working face becomes very high. (6) Cycles of pressure increase–decrease were repeated as long as the water pressure changes initiated an EMR activity. (7) When EMR activity induced by water pressure changes did not appear, water infusion was finished.

An example of EMR registration during water infusion is shown in Fig. 5. Water infusion was carried out in the drift face of Andreevsky stratum (at 700 m depth, average rock density is about of 2×10^3 kg/m^3, water increase step size is 4 MPa (0.3 γH), while maximal water pressure value is 11 MPa (maximal water pressure must be not higher than 0.8 γH, see above). DCR value measured in the drift face was 6 l/m, hence, a rockburst hazardous situation was revealed.

Fig. 5 shows that an increase of water pressure up to 4 MPa during the first cycle is associated with EMR activity excitation (500

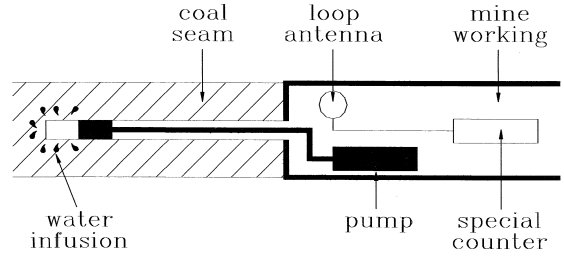

Fig. 4. Schematic diagram of experimental arrangement.

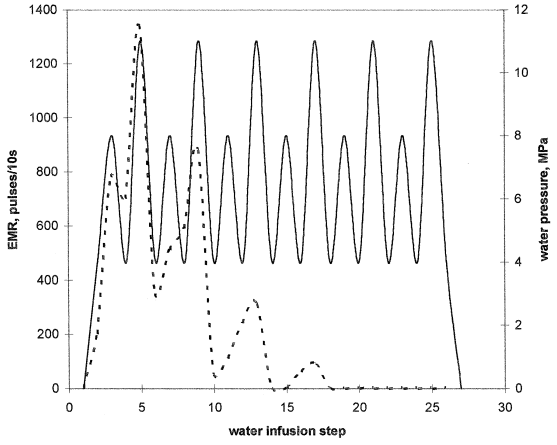

Fig. 5. An example of EMR registration during water infusion. Full-drawn curve is the water pressure, while the hatched curve is the EMR activity.

pulse/10 s); the following water pressure rise up to 8 MPa initiated an additional increase of EMR activity (about 800 pulse/10 s). A decrease of water pressure to 4 MPa elicited insignificant decrease of EMR activity, and water pressure increase up to 11 MPa resulted in an additional EMR activity burst (1350 pulse/10 s).

A decrease of water pressure to 4 MPa led to a significant decrease of EMR activity, however, its level remained high enough. Therefore, the water pressure rise during the second cycle induced an increase of EMR activity.

After the second cycle of water infusion, EMR activity decreased to 50 pulse/10 s. Drilling of a forecast borehole showed that DCR value was about 4.5 l/m. This value is a little lower than the criterion level, while it also shows that the zone of drift influence is still stressed enough.

The EMR activity was large up to the third cycle of water infusion, while the fifth and sixth cycles of water infusion were not associated with any EMR appearance. Drilling of a forecast borehole after the sixth cycle of water infusion showed that it was impossible to determine the DCR value, due to very high coal humidity. However, measurement of natural EMR activity showed that the average value of natural EMR activity was about 50 pulse/10 s, that is significantly lower than the limiting value of natural EMR activity (120 pulse/10 s, Frid, 1997b), and showed that the zone near the mine working face was non-dangerous.

Note that the absence of EMR excitation due to water pressure changes is a qualitative criterion. It does not determine, for example, the number of water pressure cycles needed for water infusion performance. In the case shown in Fig. 4, water infusion could have been finished after the fifth cycle, while the sixth cycle was superfluous. However, our research (more than 70 EMR investigations during water infusion) has showed that the EMR criterion really characterizes water infusion performance.

7. Conclusion

As is known, EMR activity is used for rockburst and coal and gas outburst forecast.

The new interdisciplinary approach consisting of rock mechanics analysis of safety condition and rigid sample deformation, and geophysical EMR investigation, both in the laboratory (during sample compression) and in situ (during borehole drilling and during a water infusion) enables us to apply EMR for water infusion performance control. The results showed that if EMR activity is lacking during a water pressure decrease–increase cycle, water infusion is really effective and the mine working face is non-hazardous.

Acknowledgements

The author would like to thank the critical review of Prof. N.B. Christensen, Prof. T. Lee, Prof. I. Yamada, the comments of which greatly improved this paper, and M. Draizner for many helpful suggestions in preparing this article.

References

Cress, G., Brady, B., Rowell, G., 1987. Sources of electromagnetic radiation from fracture of rock samples in laboratory. Geophys. Res. Lett. 14 (4), 331–334.

Enomoto, Y., Chaudhri, M., 1993. Fracto-emission during fracture of engineering ceramics. J. Am. Ceram. Soc. 76 (10), 2583–2587.

Frid, V., 1990. Rock burst forecast by electromagnetic radiation method. PhD thesis.

Frid, V., 1997a. Electromagnetic radiation method for rock and gas outburst forecast. J. Appl. Geophys. 38, 97–104.

Frid, V., 1997b. Rock-burst hazard forecast by electromagnetic radiation excited by rock fracture. J. Rock Mech. Rock Eng. 30 (4), 229–236.

Frid, V., Shabarov, A., Proskurjakov, V., 1992. Formation of electromagnetic radiation in coal stratum. J. Mining Sci. 28 (2), 139–145.

Frid, V., Rabinovitch, A., Bahat, D., 1999. Electromagnetic radiation associated with induced triaxial fracture in granite. Philos. Mag. Lett. 79, 79–84.

Fujinawa, Y., Kumagai, T., Takahashi, K., 1992. A study of anomalous underground electric field variations associated with volcanic eruption. Geophys. Res. Lett. 19 (1), 9–12.

Gershenzon, N., Zilpimiani, D., Maguladze, P., 1985. Electromagnetic radiation from crack tip during ionic crystals fracture. DAN SSSR 248, 1077–1081.

Gershenzon, N., Gokhberg, M., Karakin, A., 1989. Modeling the connection between earthquake preparation process and crystal electromagnetic emission. Phys. Earth. Planet. Enter. 57 (1–2), 129–138.

Gokhberg, M., Morgunov, V., Aronov, E., 1979. High frequency electromagnetic radiation during seismic activity. DAN SSSR 285, 75–78.

Gol'd, R.M., Markov, G., Mogila, P.G., 1975. Pulsed electromagnetic radiation of minerals and rocks subjected to mechanical loading. Izv. Earth Phys. 7, 109–111.

Golovin, Y., Shibkov, A., 1986a. Dynamics of dislocation pile-ups and pulsed polarization of LiF single crystals in the case of single slip. Sov. Phys. Solid State 28 (9), 1625–1626.

Golovin, Y., Shibkov, A., 1986b. Fast electrical processes and dynamics of dislocations in plastically deformed alkali halide crystals. Sov. Phys. Solid State 28 (11), 1965–1968.

Goncharov, A., Korjakov, V.P., Kuznetzov, V.M., 1980. Acoustic emission and electromagnetic radiation during uniaxial compression. DAN SSSR 255 (4), 821–824.

Ipatov, Y., 1989. Fundamentals of electromagnetic radiation method for rockburst forecast on Khibin apatite mines. PhD thesis.

Khatiashvili, N., 1984. The electromagnetic effect accompanying the fracturing of alkaline halide crystals and rocks. Izv. Earth Phys. 20, 656–661.

King, C., 1983. Electromagnetic emissions before earthquakes. Nature 301, 377.

Markov, G.A., Ipatov, Y., 1986. Method of electromagnetic radiation for rockburst forecast on apatite mines. Eng. Geol. 3, 54–57, in Russian.

Miroshnishenko, M., Kuksenko, V., 1980. Emission of electromagnetic pulses during nucleation of cracks in solid insulators. Sov. Phys. Solid State 22 (5), 895–896.

Nesbitt, A.C., Austin, B.A., 1988. The emission and propagation of electromagnetic energy from stressed quartzite rock underground. Trans. SA Inst. Electr. Eng. 79, 53–57.

Nitsan, V., 1977. Electromagnetic emission accompanying fracture of quartz-bearing rocks. Geotherm. Res. Lett. 4 (8), 333–335.

Ogawa, T., Oike, K., Miura, T., 1985. Electromagnetic radiation from rocks. J. Geophys. Res. 90 (d4), 6245–6251.

Perelman, M., Khatiashvilli, N., 1981. Radioemission during brittle failure. DAN SSSR 256 (4), 824–826.

Petukhov, I.M., Lin'kov, L.M., 1983. Mechanics of rock bursts and outbursts. Nedra, Moskva, in Russian.

Rabinovitch, A., Bahat, D., Frid, V., 1995. Comparison of electromagnetic radiation and acoustic emission in granite fracturing. Int. J. Fract. 71 (2), r33–r41.

Rabinovitch, A., Bahat, D., Frid, V., 1996. Emission of electromagnetic radiation by rock fracturing. Z. Geol. Wiss. 24 (3–4), 361–368.

Rabinovitch, A., Frid, V., Bahat, D., 1998. Parameterization of Electromagnetic radiation pulses obtained by triaxial fracture in granite samples. Philos. Mag. Lett. 77 (5), 289–293.

Rabinovitch, A., Frid, V., Bahat, D., 1999. A note on the amplitude–frequency relation of electromagnetic radiation pulses induced by material failure. Philos. Mag. Lett. 79, 195–200.

Red'kin, V., Kuprijanov, A.S., Bufalov, V.V., 1985. Geophysical devices for distance rock burst control. Geophysical methods of stress and deformation control, Novosibirsk, pp. 81–82, in Russian.

Scitovich, V.P., Lazarevich, L.M., 1985. Estimation of stress condition of rock massive by EMR, in: Geophysical Methods of Stress and Deformation Control, Novosibirsk, pp. 65–66, in Russian.

Twiss, R.J., Moores, E.M., 1992. Structural Geology, Freeman, NY.

Urusovskaja, A.A., 1969. Electric effects associated with plastic deformation of ionic crystals. Sov. Phys-Usp. 11, 631–643.

Warwick, J., Stoker, C., Meyer, T., 1982. Radio emission associated with rock fracture: possible application to

great Chilean Earthquake of May 22, 1960. J. Geophys. Res. 87 (B4), 2851–2859.

Xu, W., Tong, W., Wu, P., 1991. Experimental study of electromagnetic radiation during rock fracture. Adv. Geophys. Res. 2, 73–83.

Yamada, I., Masuda, K., Mizutani, H., 1989. Electromagnetic and acoustic emission associated with rock fracture. Phys. Earth Planet. Inter. 57 (1–2), 157–168.

Yoshino, T., Tomizawa, I., Sugimoto, T., 1993. Results of statistical analysis of low-frequency seismogenic EM emissions as precursors to earthquakes and volcanic eruptions. Phys. Earth Planet. Inter. 77, 21–31.